

# Does the Budyko curve reflect a maximum power state of hydrological systems? A backward analysis

M. Westhoff<sup>1</sup>, E. Zehe<sup>2</sup>, P. Archambeau<sup>1</sup>, and B. Dewals<sup>1</sup>

<sup>1</sup>Hydraulics in Environmental and Civil Engineering (HECE), University of Liege (ULg),  
Liege, Belgium

<sup>2</sup>Karlsruhe Institute of Technology (KIT), Karlsruhe, Germany

*Correspondence to:* M. Westhoff (martijn.westhoff@ulg.ac.be)

**Abstract.** Almost all catchments plot within a small envelope around the Budyko curve. This apparent behaviour suggests that organizing principles may play a role in the evolution of catchments. In this paper we applied the thermodynamic principle of maximum power as the organizing principle.

In a top-down approach we derived mathematical formulations of the relation between relative  
5 wetness and gradients driving runoff and evaporation for a simple one-box model. We did this in an  
inverse manner such that when the conductances are optimized with the maximum power principle,  
the steady state behaviour of the model leads exactly to a point on the asymptotes of the Budyko  
curve. Subsequently, we added dynamics in forcing and actual evaporations, causing the Budyko  
curve to deviate from the asymptotes. Despite the simplicity of the model, catchment observations  
10 compare reasonably well with the Budyko curves subject to observed dynamics in rainfall and actual  
evaporation. Thus by constraining the model with the asymptotes of the Budyko curve we were able  
to derive more realistic values of the aridity and evaporation index without any calibration parameter.  
Future work should focus on better representing the boundary conditions of real catchments and  
eventually adding more complexity to the model.

## 15 1 Introduction

In different climates, partitioning of rainwater into evaporation and runoff is different as well. Yet,  
when plotting the evaporation fraction against the aridity index (ratio of potential evaporation and  
rainfall), almost all catchments plot in a small envelope around a single empirical curve known as the  
Budyko curve (e.g. Gerrits et al., 2009). The fact that almost all catchments worldwide plot within  
20 this small envelope around this curve inspired several scientists to speculate whether this is due  
to co-evolution of climate and terrestrial catchment characteristics (e.g. Harman and Troch, 2014).

Co-evolution between climate and the terrestrial system could in turn be explained by an underlying organizing principle which determines optimum system functioning (Sivapalan et al., 2003; McDonnell et al., 2007; Schaeffli et al., 2011; Thompson et al., 2011; Ehret et al., 2014; Zehe et al., 25 2014). As hydrological processes are essentially dissipative, we suggest that thermodynamic optimality principles are very interesting candidates.

Belonging to this class of principles are the closely related principles of maximum entropy production (Kleidon and Schymanski, 2008; Kleidon, 2009; Porada et al., 2011; Wang and Bras, 2011; del Jesus et al., 2012; Westhoff and Zehe, 2013) and maximum power (Kleidon and Renner, 2013; 30 Kleidon et al., 2013; Westhoff et al., 2014) on the one hand – both defining the optimum configuration between competing fluxes across the system boundary – and, on the other hand, minimum energy dissipation (Rinaldo et al., 1992; Rodriguez-Iturbe et al., 1992; Hergarten et al., 2014) or maximum free energy dissipation (Zehe et al., 2010, 2013), focusing on free energy dissipation associated with changes in internal state variables as a result of boundary fluxes, i.e. soil moisture and capillary 35 potential, and a related optimum system configuration. In this research we focus on the maximum power principle.

With these principles, an optimum configuration between two competing fluxes can be determined. It seems therefore potentially suitable to derive the Budyko curve from such a principle, since the Budyko curve describes the competition between runoff and evaporation. This is also the 40 aim of this study.

The validity and the practical value of thermodynamic optimality principles are still debated (e.g. Dewar, 2009) and the partly promising results reported in the above listed studies might be just a matter of coincidence. There is a vital search for defining rigorous tests to assess how far thermodynamic optimality principles bears and applies. The Budyko curve appears very well suited for such a test, 45 as it condenses relative weights of the steady state water fluxes in most catchments around the world. It is thus not astonishing that there have been several attempts to reconcile the Budyko curve with thermodynamic optimality principles. For example, Porada et al. (2011) used the maximum entropy production principle to optimize the runoff conductance and evaporation conductance of a bucket model being forced with observed rainfall and potential evaporation of the 35 largest catchments in 50 the world. The resulting modelled fluxes were plotted in the Budyko diagram and followed the curve with a similar scatter as real world catchments.

Another very interesting approach was presented by Kleidon and Renner (2013) and Kleidon et al. (2014), using the perspective of the atmosphere. They maximized power of the vertical convective motion transporting heat and moisture upwards using the Carnot limit to constrain the sensible heat 55 flux. This motion is driven by the temperature differences between the surface and the atmosphere, while at the same time depleting this temperature gradient, leading to a maximum in power. Additionally, evaporation at the surface and condensation in the atmosphere depletes this gradient even further at the expense of more vertical moisture transport and thus more convective motion. Their

approach showed some more spreading around the Budyko curve for the same 35 catchments as  
60 used in Porada et al. (2011), but they used a simpler model that has to be forced with much less  
observations, namely solar radiation, precipitation and surface temperature.

Very recently, Wang et al. (2015) used the maximum entropy production principle to de-  
rive directly an expression for the Budyko curve. They started from the expression of  
Kleidon and Schymanski (2008) and by maximizing the entropy production of the whole system  
65 they reached the expression for the Budyko curve as formulated by Wang and Tang (2014). This is  
an intriguing result that partly contradicts the findings of Westhoff and Zehe (2013), whose study  
revealed within simulations with an HBV type conceptual model, that joint optimization of overall  
entropy production results in optimum conductances approaching zero.

The objective of this study is to define a model which, under constant forcing, leads to a point  
70 on the asymptotes of the Budyko curve when flow conductances are optimized with the maximum  
power principle. The model is comparable to the one proposed by Porada et al. (2011), but with  
different relations between relative wetness and driving gradients. We derived the gradients driving  
evaporation and runoff in an inverse manner, with both the asymptotes of the Budyko curve and  
the maximum power principle as constraints. Subsequently, we added dynamics in forcing or in  
75 actual evaporation (similar to Westhoff et al., 2014) to move away from these asymptotes to more  
realistic values of the aridity and evaporation index, without calibrating any parameter. Finally, these  
sensitivities were compared to observations.

## 2 The maximum power principle

The maximum power principle implies that a system evolves in such a way that steady state fluxes  
80 across a systems boundary produce maximum power. It is directly derived from the first and the  
second laws of thermodynamics, and is very well explained in Kleidon and Renner (e.g. 2013). Here  
we give only a short description: let us start by considering a warm and a cold reservoir, which are  
connected to each other. The warm reservoir is forced by a constant energy input  $J_{in}$  and the cold  
reservoir is cooled by a heat flux  $J_{out}$ . In steady state  $J_{in} = J_{out}$  and both reservoirs have a con-  
85 stant temperature  $T_h$  and  $T_c$ , respectively, with  $T_h > T_c$ . The heat flux between the two reservoirs  
produces entropy, which is given by:

$$\sigma = \frac{J_{out}}{T_c} - \frac{J_{in}}{T_h}. \quad (1)$$

However, instead of transferring all incoming energy to the cold reservoir, the heat gradient can also  
be used to perform work (to create other forms of free energy). This means that in steady state, the  
90 incoming energy flux  $J_{in}$  equals the outgoing energy flux  $J_{out}$  plus the rate of work  $P$  (which is  
power) performed by the system.

For given temperatures of both reservoirs, the theoretical maximum rate of work is given by the Carnot limit:

$$P_{\text{Carnot}} = J_{\text{in}} \frac{T_{\text{h}} - T_{\text{c}}}{T_{\text{h}}}. \quad (2)$$

95 Now we introduce an extra flux cooling the hot reservoir as a function of its temperature  $J_{\text{h,out}} = T_{\text{h}}$ . This flux is in competition with the flux  $J_{\text{h-c}}$  between both reservoirs, while both reduce the temperature gradient between the two reservoirs. In Eq. (2)  $J_{\text{in}}$  should then be replaced by  $J_{\text{h-c}}$ , while  $T_{\text{h}}$  and  $T_{\text{c}}$  are not fixed anymore, but a function of all fluxes. In this setting, there exist a flux  $J_{\text{h-c}}$ , maximizing power. In the extreme cases of  $J_{\text{h-c}} = 0$  and  $J_{\text{h-c}} \rightarrow \infty$ , power is zero, while for  
100 intermediate values power is larger than zero.

In hydrological settings, such as this article, power is often generated by water fluxes and is given as the product of a mass flux and the potential difference driving this flux. (Note that several authors divided this formulation by the absolute temperature, while naming it maximum entropy production: e.g. Kleidon and Schymanski, 2008; Porada et al., 2011; Westhoff and Zehe, 2013; Westhoff et al.,  
105 2014; Kollet, 2015). Although, these formulations are equivalent in isothermal circumstances, the here derived maximum power principle is, in our opinion, more sound.

In the remainder of this article we used specific water fluxes [ $\text{L T}^{-1}$ ] and potential differences  $\mu_{\text{high}} - \mu_{\text{low}}$  in meter water column [L], where the flux is given as the product of a specific conductance  $k$  [ $\text{T}^{-1}$ ] and the potential difference. We recognize that, in order to come to the same units as  
110 power, these formulations should be multiplied by the water density, gravitational acceleration and a cross-sectional area, but since we are looking for a maximum, and these parameters are constant, we can leave them out. We also use the word gradient for the potential difference  $\mu_{\text{high}} - \mu_{\text{low}}$ , where the length scale with which the difference should be divided is incorporated in the conductance. With these formulation, power is given by

$$115 \quad P = k (\mu_{\text{high}} - \mu_{\text{low}})^2 \quad (3)$$

where  $k$  is the free parameter we optimized to find a maximum in power.

### 3 Mathematical framework

Here we derive the model that, when conductances are optimized with the maximum power principle, always result in a point on the asymptotes of the Budyko curve independent of the value of the given  
120 constant atmospheric inputs (here rainfall and chemical potential of the atmosphere). To reach this, proper relations between relative wetness and gradients driving runoff and evaporation were derived, which is explained in the following.

### 3.1 Initial model setup

Our model consists of a simple reservoir being filled by rainfall  $Q_{in}$  and drained by evaporation  $E_a$  and runoff  $Q_r$ . Using the same expressions as in Kleidon and Schymanski (2008), the steady state mass balance and corresponding fluxes are expressed by

$$Q_{in} = E_a + Q_r \quad (4)$$

$$E_a = k_e (\mu_s - \mu_{atm}) \quad (5)$$

$$Q_r = k_r (\mu_s - \mu_r) \quad (6)$$

where  $\mu_s$ ,  $\mu_r$  and  $\mu_{atm}$  are the chemical potential of the soil, chemical potential of the free water surface of the nearest river and chemical potential of the atmosphere, while  $k_e$  and  $k_r$  are the specific conductances of evaporation and runoff. In these expressions,  $\mu_s$  and  $\mu_s - \mu_r$  are functions of the relative saturation  $h$  in the reservoir:

$$G_e(h) = \mu_s(h) \quad (7)$$

$$G_r(h) = \mu_s(h) - \mu_r(h) \quad (8)$$

where  $G_e(h)$  and  $G_r(h)$  can have any form as long as they are strictly monotonically increasing with increasing relative saturation. For example, Porada et al. (2011) used the van Genuchten model (van Genuchten, 1980) and gravitational potential to derive the chemical potential of the soil. However, here we will derive them in such a way that, under constant forcing, we end up exactly at the Budyko curve.

### 3.2 Backwards analysis to determine the driving gradients

#### 3.2.1 Optimum $k_e^*$ matching the Budyko curve

Let us first find an optimum conductance  $k_e^*$  leading to a point on the asymptotes of the Budyko curve  $B$ . An expression describing these asymptotes exactly is given by (adapted from Wang and Tang, 2014):

$$B = \frac{E_a}{Q_{in}} = \frac{1 + E_{pot}/Q_{in} - \sqrt{(E_{pot}/Q_{in} - 1)^2}}{2} \quad (9)$$

with  $E_{pot}$  being the potential evaporation. Now we make an important assumption to define  $E_{pot}$ : we assume that evaporation is purely described as the product of a gradient and conductance; ignoring the influence of radiation. It is assumed to be maximum when in Eqs. (5) and (8),  $\mu_s = 0$ , meaning that the relative wetness is 1, implying no water limitation. With this assumption, potential evaporation is given by  $E_{pot} = k_e^* (-\mu_{atm})$  (note that  $\mu_{atm}$  is always negative). Combining this equation with Eqs. (5), (7) and (9) results in:

$$k_e^* = \frac{Q_{in}}{(G_e(h^*) - \mu_{atm})} B(k_e^*) \quad (10)$$

where  $h^*$  is the steady state relative wetness leading to a point on the asymptotes of the Budyko  
 155 curve (note that this is the relative wetness occurring when  $k_e = k_e^*$ ).

### 3.2.2 Maximum power by evaporation

As mentioned above,  $k_e^*$  should also correspond to a maximum in power by evaporation ( $P_e$ ). We did  
 this in a backward analysis, implying that we start with defining a function  $P_e(k_e)$  which is always  
 larger than zero for  $k_e \in (0, +\infty)$  and where  $\partial P_e / \partial k_e = 0$  at  $k_e = k_e^*$ . A function satisfying these  
 160 constraints is<sup>1</sup>:

$$P_e(k_e) = k_e \frac{P_0}{k_0} e^{-\left(\frac{k_e - a}{k_0}\right)^2} \quad (11)$$

where  $P_0$  and  $k_0$  are the reference power [ $L^2 T^{-1}$ ] and reference conductance [ $T^{-1}$ ], introduced to  
 come to the correct units. In all computations they have been set to unity. Setting the derivative to  
 zero for  $k_e = k_e^*$  yields:

$$165 \quad \frac{\partial P_e}{\partial k_e} = \left(2k_e^* a - 2k_e^{*2} + k_0^2\right) \frac{P_0}{k_0^3} e^{-\left(\frac{k_e^* - a}{k_0}\right)^2} = 0 \quad (12)$$

$$\rightarrow a = k_e^* - \frac{k_0^2}{2k_e^*}$$

resulting in  $P_e(k_e) = k_e P_0 / k_0 e^{-((k_e - k_e^*) / k_0 + k_0 / (2k_e^*))^2}$ .

Combining this expression with Eqs. (3) and (7):  $P_e = k_e (G_e - \mu_{\text{atm}})^2$ ,  $G_e$  is expressed as:

$$G_e(k_e) = \pm \sqrt{\frac{P_0}{k_0} e^{-\left(\frac{k_e - k_e^*}{k_0} + \frac{k_0}{2k_e^*}\right)^2} + \mu_{\text{atm}}}. \quad (13)$$

170 Since we neglect condensation ( $G_e(k_e) - \mu_{\text{atm}} \geq 0$ ), only the positive solution remains. Inserting  
 Eq. (13) into Eq. (10) and setting  $k_e = k_e^*$  yields:

$$k_e^* = \frac{Q_{\text{in}}}{\sqrt{\frac{P_0}{k_0} e^{-\frac{k_0^2}{4k_e^{*2}}}}} B(k_e^*) \quad (14)$$

which can be solved iteratively for  $k_e^*$ .

Combining these results with the mass balance (Eqs. 4–6) yields the following expression for  
 175 runoff gradient  $G_r$  as a function of  $k_e$ :

$$G_r(k_e) = \frac{Q_{\text{in}}}{k_r} - \frac{k_e}{k_r} \sqrt{\frac{P_0}{k_0} e^{-\left(\frac{k_e - k_e^*}{k_0} + \frac{k_0}{2k_e^*}\right)^2}}. \quad (15)$$

Note that any value of  $k_r$  does lead to a point on the Budyko curve.

---

<sup>1</sup>We have also tested a the function  $P_e(k_e) = P_0 \exp\left(-((k_e - a)/k_0)^2\right)$ , but this led to two non-trivial solutions for  
 $k_e^*$ , and is thus less convenient to use than the expression in Eq. (11)

### 3.2.3 Maximum power by runoff

Although the Budyko curve does not depend on the value of  $k_r$ , an optimum  $k_r^*$  can still be found  
 180 by maximizing power by runoff. For this, the similar steps as for optimizing  $k_e$  are used, where in  
 Eqs. (11)–(13)  $k_e$  is simply replaced by  $k_r$ , resulting in a gradient for runoff as a function of  $k_r$ :

$$G_r(k_r) = \sqrt{\frac{P_0}{k_0} e^{-\left(\frac{k_r - k_r^*}{k_0} + \frac{k_0}{2k_r^*}\right)^2}} \quad (16)$$

while from the mass balance (Eqs. 4–8),  $k_r$  is given by

$$k_r = \frac{Q_{\text{in}} - [G_e(h) - \mu_{\text{atm}}]}{G_r(h)}. \quad (17)$$

185 Combining these two equations and setting  $k_r$  to  $k_r^*$  yields:

$$k_r^* = \frac{Q_{\text{in}} - k_e^* [G_e(k_e^*) - \mu_{\text{atm}}]}{\sqrt{\frac{P_0}{k_0} e^{-\frac{k_0^2}{4k_r^{*2}}}}} \quad (18)$$

which can also be solved iteratively for  $k_r^*$ .

### 3.3 Forward analysis

To apply the maximum power principle in any hydrological model, the model should run until  
 190 a (quasi)-steady state is reached. Within the above presented backward analysis the steady state  
 optimum gradients are simply found by giving  $k_e$  the value of  $k_e^*$  in Eq. (13) and  $k_r = k_r^*$  in Eq. (15).

However, when the relative wetness  $h$  evolves over time, the gradients should be resolved as  
 a function of the relative wetness ( $G_e = G_e(h)$  and  $G_r = G_r(h)$ ). To do this, we assumed that  $h$   
 is a linear function of  $G_r(k_e)$  scaled between zero and unity (for sensitivities to different initial  
 195 relations between relative wetness and one of the gradients see supplementary data):

$$G_r(h) = \min[G_r(k_e)] + (\max[G_r(k_e)] - \min[G_r(k_e)])h \quad (19)$$

where the maximum in  $G_r(k_e)$  occurs when the second term on the right-hand-side of Eq. (15)  
 is zero:  $\max[G_r(k_e)] = \frac{Q_{\text{in}}}{k_r}$  and the minimum value is derived when this second term is maximum,  
 occurring at  $k_e = k_e^{\text{max}} = 1/2 \left( k_e^* - \frac{k_0^2}{2k_e^*} + \sqrt{\left( k_e^* - \frac{k_0^2}{2k_e^*} \right)^2 + 4} \right)$ . Inserting this into Eq. (15) yields:

$$200 \quad \min[G_r(k_e)] = \frac{Q_{\text{in}}}{k_r} - \frac{k_e^{\text{max}}}{k_r} \sqrt{\frac{P_0}{k_0} e^{-\left(\frac{k_e^{\text{max}} - k_e^*}{k_0} + \frac{k_0}{2k_e^*}\right)^2}}. \quad (20)$$

If we now plot  $h$  vs.  $G_e$ , a unique relation between the two exists (Fig. 1).

With the gradients as functions of  $h$ , the non-steady mass balance equation is written as

$$S_{\text{max}} \frac{dh}{dt} = Q_{\text{in}} - k_r G_r(h) - k_e (G_e(h) - \mu_{\text{atm}}) \quad (21)$$

where  $S_{\text{max}}$  is the maximum storage depth [L] and  $t$  is time [T]. Now, the time evolution of the  
 205 relative wetness can be simulated.

## 4 Results and discussion from forward analysis

### 4.1 Constant forcing

With the known relations between relative wetness and gradients driving evaporation and runoff, the forward model was run and  $k_e$  be optimized by maximizing power. With constant forcing, each value of  $\mu_{\text{atm}}$  resulted in a point on the asymptotes of the Budyko curve (Fig. 2a). In Fig. 2b, the time evolution of the relative wetness and both gradients are shown for an initially saturated and an initially dry state indicating that irrespective of the initial state, the forward model evolves to a steady state.

### 4.2 Sensitivity to dry spells

By introducing dynamics in forcing, we expected the resulting budyko curve to deviate from the asymptotes.

In literature, the deviation from the asymptotes is often done by introducing a empirical parameter (e.g. Choudhury, 1999; Wang and Tang, 2014). To move away from this empiricism, we start at the asymptotes of the Budyko curve. Subsequently, we added dry spells and dynamics in evaporation (e.g. when trees lose their leaves the evaporative conductance  $k_e$  goes to zero) and tested how this influenced the Budyko curve.

To test sensitivities to dry spells, simple block functions were used, with either a predefined constant input or no input at all. For longer relative lengths of the dry spell, the slope of the curves becomes smaller until a maximum of  $E_a/Q_{\text{in}} = 0.98$  (Fig. 3). The reason the asymptotes do not reach unity lies in the fact that already at very short dry spells a second maximum in power evolves, while the first maximum disappears quickly with increasing dry spells. This is in line with results of Westhoff et al. (2014) while also in Zehe et al. (2013) a second optimum is present. Although interesting, we leave a better exploration of this transition zone where two maxima exist for future research.

These curves were compared with data of real catchments that have a relatively stable wet period interspersed with a regular dry period. The Mupfure catchment (Zimbabwe, Savenije, 2004) with approximately seven months without rain (Fig. S1 in the Supplement), plots very close to the theoretical curve with the same length of the dry spell. However, catchments from the MOPEX database (Schaake et al., 2006) with clear consistent dry spells plot still far from the respective theoretical curves. This discrepancy can be partly explained by the somewhat arbitrary way the number of dry months are determined: The MOPEX catchments are filtered to have only those catchments having at least one month with a median rainfall  $< 2.5 \text{ mm month}^{-1}$  and a coefficient of variance  $< 0.5$  for all months with a median rainfall  $> 25 \text{ mm month}^{-1}$ . The final number of dry months were determined maximizing the difference between the mean monthly precipitation of the  $X$  driest months minus the mean monthly precipitation of the  $1 - X$  wettest months, where  $X = 1, 2 \dots 12$ .



For example, the MOPEX catchment with a four month dry spell could also be argued to have a dry spell of seven months (Fig. S1, MOPEX ID: 11222000) and similarly, the MOPEX catchment with a five month dry spell (Fig. S1, MOPEX ID: 11210500) could also be argued to have one of six months. If these “corrections” are made, the variability within the MOPEX catchments is consistent  
245 (with longer dry spells plotting more to the right), but there is still a discrepancy of one to two months, indicating that the model should still be improved.

### 4.3 Sensitivity to dynamics in actual evaporation

We also tested the sensitivity of dynamics in actual evaporation by periodically turning  $k_e$  on and off, while keeping the rainfall constant. This sensitivity analysis shows that the longer actual evaporation  
250 is switched off, the smaller the slope of the Budyko curve and the smaller the maximum value of the evaporation index (Fig. 4). Comparing the different curves with real catchments, shows that data from the Ourthe catchment (Belgium) is relatively close to its respective line (its months without actual evaporation are estimated from Fig. 6.1 of Aalbers, 2015). Also the MOPEX catchments plot relatively close to their respective lines. However, the way the MOPEX catchments were filtered is  
255 somewhat arbitrary (only those having a coefficient of variance  $< 0.12$  for monthly median rainfall and with at least one month with a monthly median maximum ambient temperature  $< 0^\circ\text{C}$  are taken into account; a month is considered to have no actual evaporation if the monthly median maximum air temperature  $< 0^\circ\text{C}$ ; after Devlin, 1975, Fig. S2).

At first sight the comparison with data looks better than in the case of dry spells. However, all  
260 plotted catchments have an aridity index between 0.5 and 0.71 and within this range the different curves plot also close to each other. Yet, it is still somewhat surprising that the comparison is relatively good, since the modelled lines have been created by assuming a constant atmospheric demand ( $\mu_{\text{atm}}$ ) for each run, which is different from real catchments that have a more or less sinus shape potential evaporation over the year. However, we consider it as future work to better represent the  
265 real world dynamics in the model.

## 5 Conclusions and outlook

The Budyko curve is an empirical proof that only a subset of all possible combinations of aridity index and evaporation index emerges in nature. It belongs to the, so-called Darwinian models (Harman and Troch, 2014), focusing on emergent behaviour of a system as a whole. Since the maximum power principle links Newtonian models with the Darwinian models, it has indeed potential  
270 to derive the Budyko curve with an, in essence, Newtonian model.

We presented a top-down approach in which we derived relations between relative wetness and chemical potentials that lead, under constant forcing, to a point on the asymptotes of the Budyko

curve when the maximum power principle is applied. Subsequently sensitivities to dynamics in forcing and actual evaporation were tested.

Since the Budyko curve is an empirical curve, a calibration parameter is often linked to catchment specific characteristics such as land use, soil water storage, climate seasonality or spatial scales (e.g. Milly, 1994; Choudhury, 1999; Zhang et al., 2004; Potter et al., 2005). Although correlations between characteristics and the calibration parameter have been found, it remains a calibration parameter.

Here we presented a method to derive the the Budyko curve without any calibration parameter, but sensitive to temporal dynamics in boundary conditions. Although we used simple block functions to test these sensitivities they compare reasonably well with observations. Nevertheless, improvements could be made by modelling dynamics closer to reality, or even by adding multiple parallel reservoirs to account for spatial variability within a catchment.

Even though the model represents observations reasonably well (despite its simplicity), the method used here is by no means a proof that the maximum power principle does apply for hydrological systems. This is due to the top-down derivation of the gradients in which the maximum power principle is used explicitly. In principle, the method could also be used with respect to any other optimization principle. However, the reasonable fits with observations gives floor to further explore this methodology – including the maximum power principle.

**The Supplement related to this article is available online at  
doi:10.5194/hess-0-1-2015-supplement.**

*Acknowledgements.* We would like to thank Miriam Coenders-Gerrits for providing data of the Mupfure catchment, Wouter Berghuijs for his help with the MOPEX dataset and Service Public de Wallonie for providing river flow data of the Ourthe catchment. This research was supported by the University of Liege and the EU in the context of the MSCA-COFUND-BeIPD project.

## References

- Aalbers, E.: Evaporation in conceptual rainfall-runoff models: testing model realism using re-  
300 motely sensed evaporation, Master's thesis, Delft University of Technology, available at:  
<http://repository.tudelft.nl/view/ir/uuid:a2edc688-2270-4823-aa93-cb861cf481a2/>, last access: 10 Au-  
gust 2015.
- Choudhury, B.: Evaluation of an empirical equation for annual evaporation using field observations and results  
from a biophysical model, *J. Hydrol.*, 216, 99–110, doi:10.1016/S0022-1694(98)00293-5, 1999.
- 305 del Jesus, M., Foti, R., Rinaldo, A., and Rodriguez-Iturbe, I.: Maximum entropy production, carbon assimila-  
tion, and the spatial organization of vegetation in river basins, *P. Natl. Acad. Sci. USA*, 109, 20837–20841,  
doi:10.1073/pnas.1218636109, 2012.
- Devlin, R.: *Plant Physiology*, 3rd Edn., D. Van Nostrand Company, New York, 1975.
- Dewar, R. C.: Maximum Entropy Production as an Inference Algorithm that Translates Physical Assumptions  
310 into Macroscopic Predictions: Don't Shoot the Messenger, *Entropy*, 11, 931–944, doi:10.3390/e11040931,  
2009.
- Ehret, U., Gupta, H. V., Sivapalan, M., Weijs, S. V., Schymanski, S. J., Blöschl, G., Gelfan, A. N., Harman, C.,  
Kleidon, A., Bogaard, T. A., Wang, D., Wagener, T., Scherer, U., Zehe, E., Bierkens, M. F. P., Di Baldas-  
sarre, G., Parajka, J., van Beek, L. P. H., van Griensven, A., Westhoff, M. C., and Winsemius, H. C.: Ad-  
315 vancing catchment hydrology to deal with predictions under change, *Hydrol. Earth Syst. Sci.*, 18, 649–671,  
doi:10.5194/hess-18-649-2014, 2014.
- Gerrits, A. M. J., Savenije, H. H. G., Veling, E. J. M., and Pfister, L.: Analytical derivation of the Budyko  
curve based on rainfall characteristics and a simple evaporation model, *Water Resour. Res.*, 45, W04403,  
doi:10.1029/2008WR007308, 2009.
- 320 Harman, C. and Troch, P. A.: What makes Darwinian hydrology “Darwinian”? Asking a different kind of  
question about landscapes, *Hydrol. Earth Syst. Sci.*, 18, 417–433, doi:10.5194/hess-18-417-2014, 2014.
- Hergarten, S., Winkler, G., and Birk, S.: Transferring the concept of minimum energy dissipation from river net-  
works to subsurface flow patterns, *Hydrol. Earth Syst. Sci.*, 18, 4277–4288, doi:10.5194/hess-18-4277-2014,  
2014.
- 325 Kleidon, A.: Nonequilibrium thermodynamics and maximum entropy production in the Earth system, *Natur-  
wissenschaften*, 96, 653–677, doi:10.1007/s00114-009-0509-x, 2009.
- Kleidon, A. and Renner, M.: Thermodynamic limits of hydrologic cycling within the Earth system: concepts,  
estimates and implications, *Hydrol. Earth Syst. Sci.*, 17, 2873–2892, doi:10.5194/hess-17-2873-2013, 2013.
- Kleidon, A. and Schymanski, S.: Thermodynamics and optimality of the water budget on land: a review, *Geo-  
330 phys. Res. Lett.*, 35, L20404, doi:10.1029/2008GL035393, 2008.
- Kleidon, A., Zehe, E., Ehret, U., and Scherer, U.: Thermodynamics, maximum power, and the dynam-  
ics of preferential river flow structures at the continental scale, *Hydrol. Earth Syst. Sci.*, 17, 225–251,  
doi:10.5194/hess-17-225-2013, 2013.
- Kleidon, A., Renner, M., and Porada, P.: Estimates of the climatological land surface energy and  
335 water balance derived from maximum convective power, *Hydrol. Earth Syst. Sci.*, 18, 2201–2218,  
doi:10.5194/hess-18-2201-2014, 2014.

- Kollet, S. J.: Optimality and inference in hydrology from entropy production considerations: synthetic hillslope numerical experiments, *Hydrol. Earth Syst. Sci. Discuss.*, 12, 5123–5149, doi:10.5194/hessd-12-5123-2015, 2015.
- 340 McDonnell, J., Sivapalan, M., Vaché, K., Dunn, S., Grant, G., Haggerty, R., Hinz, C., Hooper, R., Kirchner, J., Roderick, M., Selker, J., and Weiler, M.: Moving beyond heterogeneity and process complexity: a new vision for watershed hydrology, *Water Resour. Res.*, 43, W07301, doi:10.1029/2006WR005467, 2007.
- Milly, P. C. D.: Climate, soil water storage, and the average annual water balance, *Water Resour. Res.*, 30, 2143–2156, doi:10.1029/94WR00586, doi:10.1029/94WR00586, 1994.
- 345 Porada, P., Kleidon, A., and Schymanski, S. J.: Entropy production of soil hydrological processes and its maximisation, *Earth Syst. Dynam.*, 2, 179–190, doi:10.5194/esd-2-179-2011, 2011.
- Potter, N. J., Zhang, L., Milly, P. C. D., McMahon, T. A., and Jakeman, A. J.: Effects of rainfall seasonality and soil moisture capacity on mean annual water balance for Australian catchments, *Water Resour. Res.*, 41, w06007, doi:10.1029/2004WR003697, 2005.
- 350 Rinaldo, A., Rodriguez-Iturbe, I., Rigon, R., Bras, R. L., Ijjasz-Vasquez, E., and Marani, A.: Minimum energy and fractal structures of drainage networks, *Water Resour. Res.*, 28, 2183–2195, doi:10.1029/92WR00801, 1992.
- Rodriguez-Iturbe, I., Rinaldo, A., Rigon, R., Bras, R. L., Ijjasz-Vasquez, E., and Marani, A.: Fractal structures as least energy patterns: The case of river networks, *Geophys. Res. Lett.*, 19, 889–892, doi:10.1029/92GL00938, 355 1992.
- Savenije, H. H. G.: The importance of interception and why we should delete the term evapotranspiration from our vocabulary, *Hydrol. Process.*, 18, 1507–1511, doi:10.1002/hyp.5563, 2004.
- Schaake, J., Cong, S., and Duan, Q.: The US MOPEX data set, *IAHS-AISH P.*, 307, 9–28, 2006.
- Schaefli, B., Harman, C. J., Sivapalan, M., and Schymanski, S. J.: HESS Opinions: Hydrologic pre- 360 dictions in a changing environment: behavioral modeling, *Hydrol. Earth Syst. Sci.*, 15, 635–646, doi:10.5194/hess-15-635-2011, 2011.
- Sivapalan, M., Blöschl, G., Zhang, L., and Vertessy, R.: Downward approach to hydrological prediction, *Hydrol. Process.*, 17, 2101–2111, 2003.
- Thompson, S., Harman, C., Troch, P., Brooks, P., and Sivapalan, M.: Spatial scale dependence of ecohydrologi- 365 cally mediated water balance partitioning: a synthesis framework for catchment ecohydrology, *Water Resour. Res.*, 47, W00J03, doi:10.1029/2010WR009998, 2011.
- van Genuchten, M. T.: A closed-form equation for predicting the hydraulic conductivity of unsaturated soils, *Soil Sci. Soc. Am. J.*, 44, 892–898, doi:10.2136/sssaj1980.03615995004400050002x, 1980.
- Wang, D. and Tang, Y.: A one-parameter Budyko model for water balance captures emergent behavior in dar- 370 winian hydrologic models, *Geophys. Res. Lett.*, 41, 4569–4577, doi:10.1002/2014GL060509, 2014.
- Wang, D., Zhao, J., Tang, Y., and Sivapalan, M.: A thermodynamic interpretation of Budyko and L'vovich formulations of annual water balance: proportionality hypothesis and maximum entropy production, *Water Resour. Res.*, 51, 3007–3016, doi:10.1002/2014WR016857, 2015.
- Wang, J. and Bras, R. L.: A model of evapotranspiration based on the theory of maximum entropy production, 375 *Water Resour. Res.*, 47, W03521, doi:10.1029/2010WR009392, 2011.

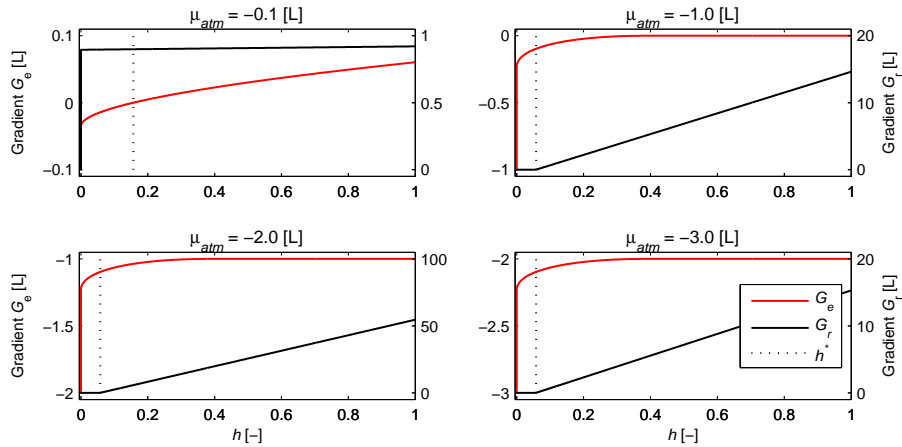


**Figure 1.** The gradients driving evaporation ( $G_e$ ) and runoff ( $G_r$ ) as a function of the relative saturation ( $h$ ) for different values of  $\mu_{atm}$  with  $k_r = k_r^*$  and  $n = 2$ . At  $h = 0$ , the slope of the gradient  $G_e$  is vertical, while the value of  $G_r$  is set to zero to avoid runoff at zero saturation.

Westhoff, M. C. and Zehe, E.: Maximum entropy production: can it be used to constrain conceptual hydrological models?, *Hydrol. Earth Syst. Sci.*, 17, 3141–3157, doi:10.5194/hess-17-3141-2013, 2013.

Westhoff, M. C., Zehe, E., and Schymanski, S. J.: Importance of temporal variability for hydrological predictions based on the maximum entropy production principle, *Geophys. Res. Lett.*, 41, 67–73, doi:10.1002/2013GL058533, 2014.

Yang, H., Yang, D., Lei, Z., and Sun, F.: New analytical derivation of the mean annual water-energy balance equation, *Water Resour. Res.*, 44, W03410, doi:10.1029/2007WR006135, 2008.

Zehe, E., Blume, T., and Blöschl, G.: The principle of “maximum energy dissipation”: a novel thermodynamic perspective on rapid water flow in connected soil structures, *Philos. T. R. Soc. B*, 365, 1377–1386, doi:10.1098/rstb.2009.0308, 2010.

Zehe, E., Ehret, U., Blume, T., Kleidon, A., Scherer, U., and Westhoff, M.: A thermodynamic approach to link self-organization, preferential flow and rainfall–runoff behaviour, *Hydrol. Earth Syst. Sci.*, 17, 4297–4322, doi:10.5194/hess-17-4297-2013, 2013.

Zehe, E., Ehret, U., Pfister, L., Blume, T., Schröder, B., Westhoff, M., Jackisch, C., Schymanski, S. J., Weiler, M., Schulz, K., Allroggen, N., Tronicke, J., van Schaik, L., Dietrich, P., Scherer, U., Eccard, J., Wulfmeyer, V., and Kleidon, A.: HESS Opinions: From response units to functional units: a thermodynamic reinterpretation of the HRU concept to link spatial organization and functioning of intermediate scale catchments, *Hydrol. Earth Syst. Sci.*, 18, 4635–4655, doi:10.5194/hess-18-4635-2014, 2014.

Zhang, L., Hickel, K., Dawes, W. R., Chiew, F. H. S., Western, A. W., and Briggs, P. R.: A rational function approach for estimating mean annual evapotranspiration, *Water Resour. Res.*, 40, w02502, doi:10.1029/2003WR002710, 2004.

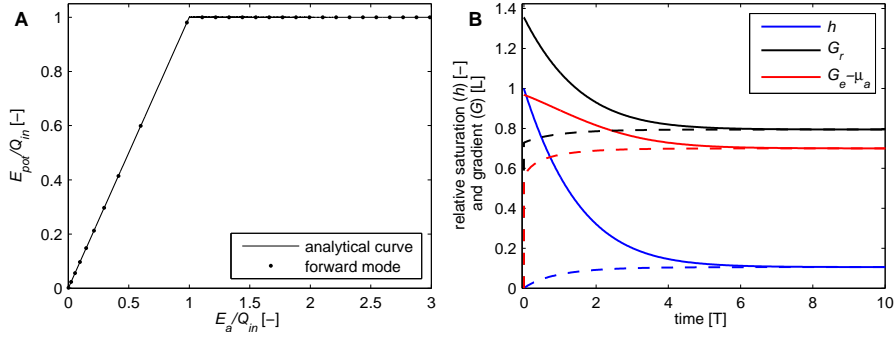


**Figure 2.** (a) Analytical Budyko curve (Eq. 9) and result from forward mode with constant forcing and (b) time evolution of relative saturation and both gradients for complete initial saturation (solid lines) and initial dry state (dashed lines).  $\mu_{atm} = -0.7$ .

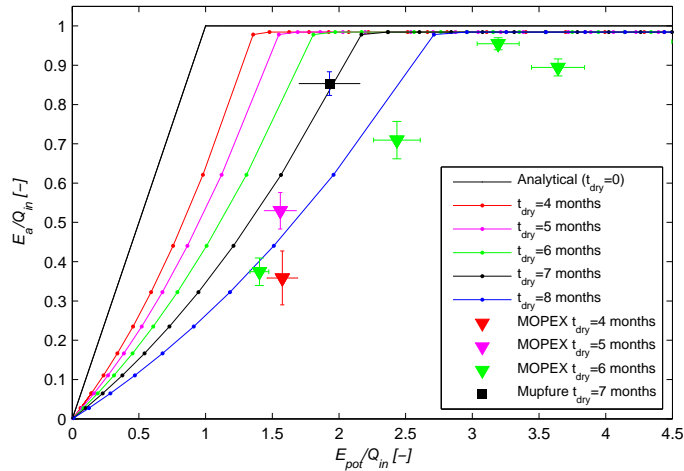


**Figure 3.** Sensitivity to periodic dry spells to the forward model. MOPEX catchments are filtered to have only those catchments having at least one month with a median rainfall  $< 2.5 \text{ mm month}^{-1}$  and a coefficient of variance  $< 0.5$  for all months with a median rainfall  $> 25 \text{ mm month}^{-1}$ . The final number of dry months were determined maximizing the difference between the mean monthly precipitation of the  $X$  driest months minus the mean monthly precipitation of the  $1 - X$  wettest months, where  $X = 1, 2 \dots 12$ . Error bars indicate one standard deviation and are determined with bootstrap sampling.

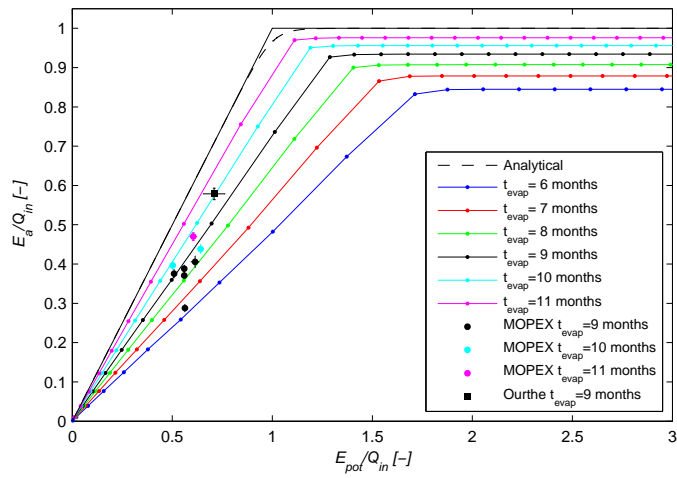


**Figure 4.** Sensitivity to on-off dynamics in actual evaporation to the forward model. MOPEX catchments were filtered to have only those catchments having a coefficient of variance  $< 0.12$  for monthly median rainfall and with at least one month with a median maximum air temperature  $< 0^\circ\text{C}$ ; a month is considered to have no actual evaporation if the monthly median maximum air temperature  $< 0^\circ\text{C}$  (after Devlin, 1975). Error bars indicate one standard deviation and are determined with bootstrap sampling.